Mechanism of the Antichaperone Activity of Protein Disulfide Isomerase: Facilitated Assembly of Large, Insoluble Aggregates of Denatured Lysozyme and PDI†

Vera Sideraki and Hiram F. Gilbert*

Verna and Marrs McLean Department of Biochemistry, Baylor College of Medicine, Houston, Texas 77030

Received September 27, 1999; Revised Manuscript Received December 2, 1999

ABSTRACT: Protein disulfide isomerase (PDI), a folding catalyst and chaperone can, under certain conditions, facilitate the misfolding and aggregation of its substrates. This behavior, termed antichaperone activity [Puig, A., and Gilbert, H. F., (1994) *J. Biol. Chem. 269*, 25889] may provide a common mechanism for aggregate formation in the cell, both as a normal consequence of cell function or as a consequence of disease. When diluted from the denaturant, reduced, denatured lysozyme (10−50 μM) remains soluble, although it does aggregate to form an ensemble of species with an average sedimentation coefficient of 23 ± 5 S (∼600 ± 100 kDa). When low concentrations of PDI (1−5 μM) are present, the majority (80 ± 8%) of lysozyme molecules precipitate in large, insoluble aggregates, together with 87 ± 12% of the PDI. PDI-facilitated aggregation occurs even when disulfide formation is precluded by the presence of dithiothreitol (10 mM). Maximal lysozyme−PDI precipitation occurs at a constant lysozyme/PDI ratio of 10:1 over a range of lysozyme concentrations (10−50 μM). Concomitant resolubilization of PDI and lysozyme from these aggregates by increasing concentrations of urea suggests that PDI is an integral component of the mixed aggregate. PDI induces lysozyme aggregation by noncovalently cross-linking 23 S lysozyme species to form aggregates that become so large (∼38 000 S) that they are cleared from the analytical ultracentrifuge even at low speed (1500 rpm). The rate of insoluble aggregate formation increases with increasing PDI concentration (although a threshold PDI concentration is observed). However, increasing lysozyme concentration slows the rate of aggregation, presumably by depleting PDI from solution. A simple mechanism is proposed that accounts for these unusual aggregation kinetics as well as the switch between antichaperone and chaperone behavior observed at higher concentrations of PDI.

Aggregation, a nonproductive fate for proteins that are in the process of folding, has been implicated in the etiology of several diseases. The amyloid diseases (Alzheimer's, Parkinson's, Huntington's disease, familial amyloid polyneuropathy, and the prion diseases) have all been linked to the aberrant folding of normally soluble proteins. Aggregation in this case leads to the deposition of β-sheet-containing fibrillar aggregates (*1*−*3*). The normal, native structures of amyloidogenic proteins are extremely variable, presenting few clues as to what triggers amyloidogenesis in vivo (*1*). Point mutations can increase the rate of fibrillization in vitro (*4*) and/or decrease the stability of the native fold (*5*, *6*). Although the formation of the cross-β scaffold motif by specific folding intermediates is an accepted mechanism for amyloid fibrillogenesis (*7*), amorphous aggregates may serve as amyloidogenic intermediates (*8*). Chaperones and other cellular proteins may also facilitate the formation of insoluble aggregates (*2*). For example, the transformation of the cellular form of the prion-protein to the infectious state involves another cellular protein, protein X (*3*). Inheritance of the prion-like Ψ factor in yeast requires the participation of a molecular chaperone, hsp104 (*9*). The search for the direct involvement of molecular or pathological chaperones in amyloidogenesis continues (*10*−*12*).

Molecular chaperones suppress aggregation during protein refolding (*13*) by binding unfolded or misfolded chains or by unfolding molecules that are trapped in kinetically stable, misfolded states (*13*). However, under certain circumstances, chaperones may also participate in aggregate formation (*14*−*18*). The unusual enhancement of aggregation by a molecular chaperone has been studied most extensively for protein disulfide isomerase (PDI)[1], a very abundant component of the eukaryotic ER (*19*−*22*). PDI can influence the folding process in three ways, depending on its concentration and whether its substrate is aggregation-prone or soluble. With substrates that are not aggregation-prone, PDI can accelerate folding by catalysis of slow thiol−disulfide exchange reactions (isomerase activity). With aggregation-prone substrates, PDI can inhibit or facilitate further substrate aggregation. At high concentrations relative to substrate, PDI is a chaperone—it inhibits aggregation and increases the yield of native protein (*19*, *20*, *22*). However, at substoichiometric concentrations, PDI facilitates substrate aggregation and

† Supported by NIH Grant GM-40379.

* To whom correspondence should be addressed: H. F. Gilbert, Department of Biochemistry, Baylor College of Medicine, One Baylor Plaza, Houston, TX 77030. Telephone: (713)798-5880. Fax: (713)-796-9438. E-mail:hgilbert@bcm.tmc.edu.

[1] Abbreviations: PDI, protein disulfide isomerase; DTT, dithiothreitol; GSH, glutathione; GSSG, glutathione disulfide.

10.1021/bi992246q CCC: $19.00
Published on Web 01/14/2000

impedes productive folding. PDI participates directly in aggregate formation and is incorporated into the aggregates (*19*, *20*). This behavior has been termed antichaperone activity.

Antichaperone activity is also observed using the other major chaperone of the ER, BiP (*21*). Like PDI, BiP promotes the formation of lysozyme aggregates when present at low concentrations relative to the refolding protein. Moreover, BiP competes with PDI for a limited number of sites within the mixed lysozyme−chaperone aggregates. This antichaperone behavior toward the refolding of lysozyme is a specific phenomenon; other proteins, such as BSA, native RNase, and phosphorylase *b*, do not significantly increase or decrease lysozyme recovery at concentrations comparable to PDI (*20*).

The participation of chaperones in aggregate formation may be part of an important physiological phenomenon. When the folding capacity of the cell is perturbed, as during protein overexpression, ATP-depletion, or redox imbalance, proteins are retained in the ER in the form of disulfide-linked, or reduced, aggregates (*23*−*26*). Aggregates and misfolded proteins are often associated with BiP (*23*, *24*) or PDI (*27*). Upon restoration of the proper ATP or redox state, ER aggregates can be correctly folded and processed (*24*, *25*). Antichaperone activity may have evolved in order to retain misfolded or unfolded proteins in the ER until such time as normal physiological conditions are restored.

In the following experiments, the mechanism by which PDI enhances hen egg white lysozyme aggregation is examined in detail. Lysozyme is an appropriate substrate for these experiments, because refolding and aggregation compete with each other kinetically (*28*−*32*). In addition, mutants of human lysozyme, implicated in hereditary amyloidosis (*33*) are capable of amyloidogenesis in vitro (*6*, *34*).

Our results show that PDI as an antichaperone specifically enhances the formation of extremely large, mixed PDI−lysozyme aggregates, which rapidly grow to a size that will precipitate out of solution. An ensemble of lysozyme aggregates (23 ± 5 S) appear to be intermediates in the process, and PDI cross-links these aggregates into a large, insoluble network. Because free PDI and free lysozyme (23 S) are both necessary to generate new cross-links that promote aggregate growth, high concentrations of either species inhibit aggregation. This mechanism accounts for chaperone and antichaperone behavior.

METHODS AND MATERIALS

Materials. Recombinant rat protein disulfide isomerase was expressed in *E. coli* and purified as previously described (*35*). GSH, GSSG, DTT, hen egg white lysozyme, and *Micrococcus lysodeicticus* cells were from Sigma. Urea was from Curtin Matheson Scientific. Gel electrophoresis reagents were from Bio-Rad.

Lysozyme Denaturation. Lysozyme (100 mg/mL) was reduced and denatured by incubating in denaturing buffer (8 M urea, 0.13 M β-mercaptoethanol, 25 mM Tris-HCl, pH 8.6) at 37 °C for 2 h. The denaturation−reduction reaction was quenched by dilution of lysozyme with 0.1 M CH_3-COOH, pH 4.0, to a final concentration of 100 μM (*19*).

Lysozyme Aggregation−Renaturation. Reduced, denatured lysozyme (100 μM) was diluted to a final concentration of 10−50 μM into 100 mM HEPES, 20 mM NaCl, 2 mM EDTA, 5 mM $MgCl_2$, pH 7.0, containing various concentrations of PDI. When disulfide formation was permitted, the redox state was maintained by a glutathione redox buffer consisting of 5 mM GSH and 0.5 mM GSSG. To inhibit disulfide formation, 10 mM dithiothreitol (DTT) was substituted for the redox buffer. Renaturation or aggregate formation was allowed to proceed overnight to ensure completion (*19*). Siliconized Eppendorf tubes (CEL Associates Inc., Houston, TX) were used in all experiments to minimize protein adsorption.

Lysozyme Activity Measurements. Lysozyme activity was measured by following the hydrolysis of *M. lysodeicticus* cells at pH 6.2 (60 mM phosphate, 0.1% NaCl) as a decrease in absorbance at 650 nm at 25 °C on a Beckman DU70 spectrophotometer. Protein concentrations were determined by the method of Bradford (*36*).

Lysozyme Solubility Assay. Insoluble aggregates were pelleted in a microcentrifuge, at 10 000 rpm (9000*g*) for 8 min and separated from soluble material. The PDI and lysozyme in the supernatant and pellet were separated by reducing SDS-PAGE, stained with Coommassie blue, and the band intensities quantitated using the Kodak Digital Science Image Analysis Software.

Aggregate Resolubilization Experiments. The insoluble material formed by incubating 10 μM lysozyme and 1 μM PDI as described above was isolated by centrifugation in a microfuge. The pellet was resuspended in various concentrations of urea (in 25 mM Tris-HCl, pH 8.6). After three rounds of vortex mixing, the solution was incubated at room-temperature overnight. After incubation with urea, the residual insoluble material and supernatants were isolated by centrifugation in a microfuge (10 000 rpm for 8 min), then quantitated by SDS-PAGE and densitometry.

Analytical Ultracentrifugation. Sedimentation velocity experiments were performed on a Beckman XL-A analytical ultracentrifuge equipped with a An60Ti rotor at 25 °C. Reduced, denatured lysozyme was diluted (10−50 μM final concentration) into buffer containing 100 mM HEPES, 20 mM NaCl, 2 mM EDTA, 5 mM $MgCl_2$, pH 7.0, 10 mM DTT, and various amounts of PDI (400 μL total volume). The time lapsed between mixing and the first scan was 2.5 min. To follow the formation of very large aggregates, samples were initially centrifuged at 1500 rpm (162*g*) and 10−20 scans were accumulated. After a stable absorbance was obtained throughout the ultracentrifuge cell, the rotor speed was increased to 42 000 rpm (127000*g*) and 30 more scans were obtained to observe the sedimentation of "soluble aggregates."

Rates of aggregation were determined during the 1500 rpm spin by monitoring the absorbance at 280 nm at a specific position in the cuvette (6.3 cm). Plots of absorbance vs time were fitted as first-order exponential decays using the Origin (Microcal) software. Sedimentation coefficients were computed using the second moment method with a specially designed version of Origin (Microcal). The sedimentation coefficients are reported in Svedbergs (S, 10^{-13} *s*). Because of light scattering of the very large aggregates, the sedimentation coefficients are only crude estimates and represent a lower limit. Average molecular weight was calculated from the sedimentation coefficients assuming a spherical particle shape using the relationship MW = 6000 $s^{3/2}$ (*37*).

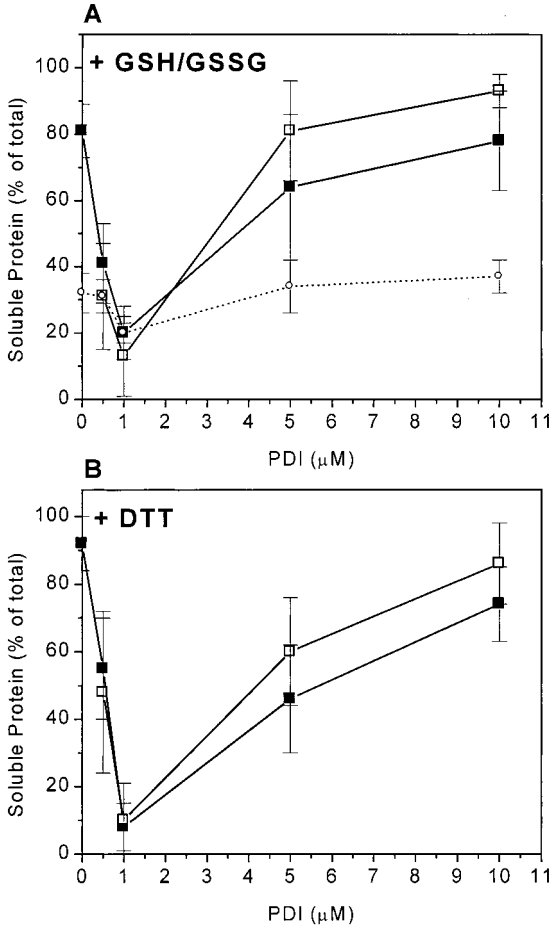

FIGURE 1: The effect of various amounts of PDI on lysozyme and PDI solubility. Reduced, denatured lysozyme (10 μM final concentration) was added to the indicated concentration of PDI at pH 7.0 (100 mM HEPES, 20 mM NaCl, 2 mM EDTA, 5 mM $MgCl_2$) and incubated overnight at room temperature before activity or solubility measurements. (A) Incubations included a glutathione redox buffer (5 mM GSH/0.5 mM GSSG). (B) Disulfide formation was inhibited by including 10 mM DTT. Activity and solubility measurements were made as described in the text. The percent solubility was based on the total amount of lysozyme. The recovery of lysozyme activity (%) was based on the activity of the same amount of native lysozyme incubated under the same conditions. (■), lysozyme solubility; (□), PDI solubility; (- - -), lysozyme activity. The error bars represent the standard deviations from multiple independent experiments.

RESULTS

Although one might expect a folding assistant to assist folding, we (*19*, *20*, *38*) and others (*22*) have previously found that at low concentrations, PDI actually facilitates lysozyme aggregation (antichaperone behavior). It facilitates refolding only at high, superstoichiometric concentrations (chaperone behavior) (*19*, *20*, *38*). After adding reduced, denatured lysozyme to a solution containing various concentrations of PDI, soluble and insoluble fractions were isolated by centrifugation and quantitated by SDS-PAGE (Figure 1A). In these experiments, disulfide formation was permitted by including a glutathione redox buffer (5 mM GSH, 0.5 mM GSSG). In the absence of PDI, most (81 ± 8%) of the lysozyme remains soluble, although only 32 ± 6% regains enzyme activity. At low concentrations, increasing PDI decreases the amount of native lysozyme formed (dotted line) and decreases the solubility of both lysozyme

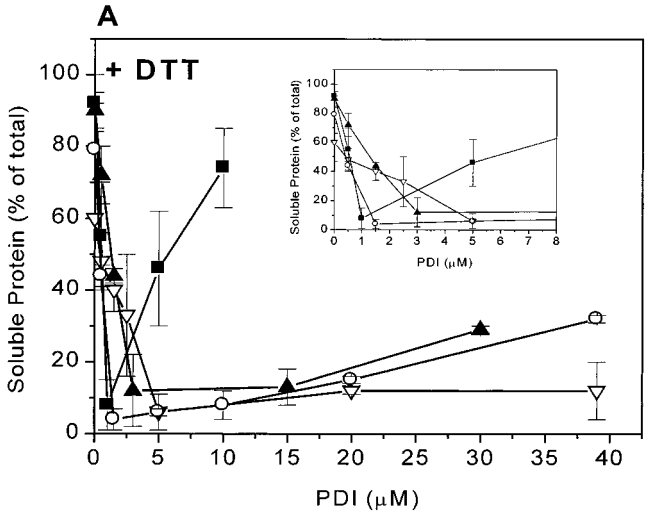

FIGURE 2: PDI demonstrates antichaperone activity at various lysozyme concentrations. The solubility of PDI and lysozyme was determined after adding reduced, denatured lysozyme to PDI in 100 mM HEPES, 20 mM NaCl, 2 mM EDTA, 5 mM $MgCl_2$, pH 7.0, buffer containing 10 mM DTT to prevent disulfide formation. The total lysozyme concentration was: (■), 10 μM; (○), 20 μM; (▲), 30 μM; (▽), 50 μM lysozyme. Inset: The scale is expanded to show that the minimum in solubility occurs at a 10:1 lysozyme/PDI ratio independently of the concentration of lysozyme. Results are from multiple, independent experiments, and error bars represent the standard deviation.

(closed symbols) and PDI (open symbols). The solubility of both proteins reaches a minimum at 1 μM PDI (with 10 μM lysozyme). At the point of minimum solubility, only 20 ± 8% of the total lysozyme is soluble, and this is all due to the small amount of enzymatically active lysozyme that is formed. The rest of the lysozyme (80%) is found in the pellet, along with all (87 ± 12%) of the PDI. Further increases in the PDI concentration increase the solubility of both proteins and increase the yield of native lysozyme.[2] The parallel between lysozyme and PDI solubility suggests that both the antichaperone and chaperone behavior of PDI arise from the effects of PDI on lysozyme aggregation. Identical experiments conducted in the presence of 10 mM DTT to inhibit disulfide formation show similar effects of PDI concentration on lysozyme and PDI solubility (Figure 1B). Even without the ability to form disulfides, PDI as an antichaperone clearly decreases the amount of soluble lysozyme and facilitates its incorporation into insoluble aggregates that also contain PDI. Thus, noncovalent forces between PDI and lysozyme are responsible for the insolubility.

Figure 2 shows the effect of PDI on lysozyme solubility as a function of the total concentration of reduced, denatured lysozyme (10 mM DTT). The antichaperone effect of PDI is clearly observed at all lysozyme concentrations examined (10−50 μM). As the lysozyme concentration increases, it takes a higher concentration of PDI to reach the solubility minimum and a higher concentration of PDI to begin to exhibit chaperone behavior (increasing solubility). In all cases, the solubility minimum is at or very close to a lysozyme to PDI ratio of 10:1 (Figure 2, inset) at all lysozyme concentrations studied. The fixed ratio of lysozyme to PDI in these large, insoluble aggregates shows that on

[2] Approximately one 100-fold more PDI is required to fully restore lysozyme activity (*19*).

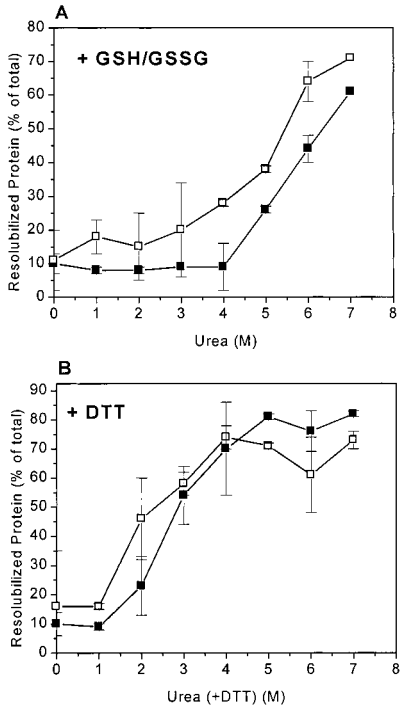

FIGURE 3: Urea resolubilizes mixed lysozyme−PDI aggregates. Lysozyme/PDI aggregates were formed under conditions described in the legend to Figure 1 using reduced, denatured lysozyme (10 μM final concentration) incubated with 1 μM PDI overnight in 100 mM HEPES, 20 mM NaCl, 2 mM EDTA, 5 mM $MgCl_2$, pH 7.0, with either 5 mM GSH/0.5 mM GSSG (Panel A) or 10 mM DTT (Panel B). Soluble and insoluble fractions were separated by centrifugation in a microfuge at 10 000 rpm for 8 min; insoluble fractions were incubated in various concentrations of urea as described in Materials and Methods. Resolubilized lysozyme (■); resolubilized PDI (□). Percent soluble protein refers to percent of initial aggregate that was resolubilized by urea or urea−DTT. Error bars represent the standard deviation from three indepedent experiments.

average, the PDI−lysozyme aggregates have a defined stoichiometry, at least at the solubility minimum, and that this stoichiometry does not vary appreciably over a relatively large range of lysozyme concentrations.

Both PDI and lysozyme are integral components of the large, insoluble aggregates that form at the solubility minimum. Insoluble aggregates were formed under redox (5 mM GSH, 0.5 mM GSSG) or reducing conditions at a lysozyme to PDI ratio that ensured maximal aggregation (10 μM lysozyme, 1 μM PDI). The mixed aggregates were then incubated in various concentrations of urea, and the resolubilized protein was measured by SDS-PAGE and densitometry. As Figure 3 shows, increasing concentrations of urea solubilize more and more of the protein. However, at each urea concentration, lysozyme and PDI are solubilized to a similar extent, within experimental error. This suggests that PDI and lysozyme are integral components of the same relatively homogeneous network rather than independent aggregates, although the variability in the experimental measurements does not preclude some aggregate heterogeneity. Aggregates formed under conditions that allow disulfide formation are highly cross-linked by disulfides (*20* and data not shown). These aggregates require higher urea concentrations to become resolubilized than aggregates formed in DTT (compare Figure 3A and B). Disulfide cross-links render the PDI−lysozyme aggregates more resistant to solubilization, but they do not provide the driving force for aggregate formation.

Repeated attempts to regain enzymatically active lysozyme from these aggregates under mild conditions were unsuccessful. Incubation with high urea concentrations was the only way to resolubilize mixed PDI−lysozyme to any significant extent. When mixed aggregates (10 μM lysozyme, 1 μM PDI) were incubated in excess PDI (5−10 μM), no significant resolubilization was seen (data not shown), whether a glutathione redox buffer or excess DTT were included with the PDI. Evidently, the lysozyme within the mixed aggregates is incorporated in a misfolded form that requires strong denaturing conditions to become soluble.

The sedimentation properties of the aggregates that are formed between lysozyme and PDI can be observed in the analytical ultracentrifuge (Figure 4). After diluting reduced, denatured lysozyme into 10 mM DTT, centrifugation at a very low speed (1500 rpm, 162*g*) fails to sediment any large, insoluble aggregates (Figure 4A). However, increasing the speed to 42 000 rpm (127000*g*) shows that much of the lysozyme is present in an ensemble of large, soluble aggregates (Figure 4B) with sedimentation coefficients between 19 and 28 S (average 23 ± 5 S). A *t*-test on replicate determinations at several lysozyme concentrations between 10 and 50 μM shows that the average *s* value does not vary significantly with lysozyme concentration. At all concentrations examined (10−50 μM), most of the lysozyme is present in these species. Assuming a spherical shape, a 23 S lysozyme aggregate would have an approximate molecular mass of 600 ± 100 kDa and would contain 30−50 lysozyme molecules, noncovalently linked. For purposes of discussion, the 23 S ensemble of lysozyme aggregates will be denoted as "soluble aggregates" to distinguish them from the large, insoluble aggregates that sediment at low speeds (1500 rpm).

Low concentrations of PDI dramatically affect lysozyme sedimentation (Figure 4). At low speed (1500 rpm, Figure 4C), the absorbance at 280 nm is initially high, presumably due to light scattering from the very large aggregates that form. The significant decrease in absorbance at the bottom of the cell between scans shows that very large aggregates are forming with time and that they are growing to a sufficient size to sediment out of the optical path between successive scans. The sedimenting material that can be observed at 1500 rpm has a very large sedimentation coefficient (Table 1). When the rotor speed is increased to 42 000 rpm (Figure 4D), the remainder of the lysozyme sediments as soluble aggregates (23 S).

There are four stages during the sedimentation experiment where different-sized species can be distinguished. Figure 5 shows how material partitions into these size classes as a function of PDI concentration. Insoluble aggregates (filled squares) form with time after mixing lysozyme and PDI. They are extremely large and sediment through the cell at a rotor speed of 1500 rpm. The amount of lysozyme that forms insoluble aggregates can be determined from the A_{280} difference between a soluble lysozyme control (no PDI) and the residual absorbance near the top of the cell after all insoluble aggregates have been cleared at 1500 rpm. In the absence of PDI, practically no lysozyme molecules are incorporated into insoluble aggregates. During the time the rotor speed is increased from 1500 to 42 000 rpm, there is some sedimentation of material that can be detected from

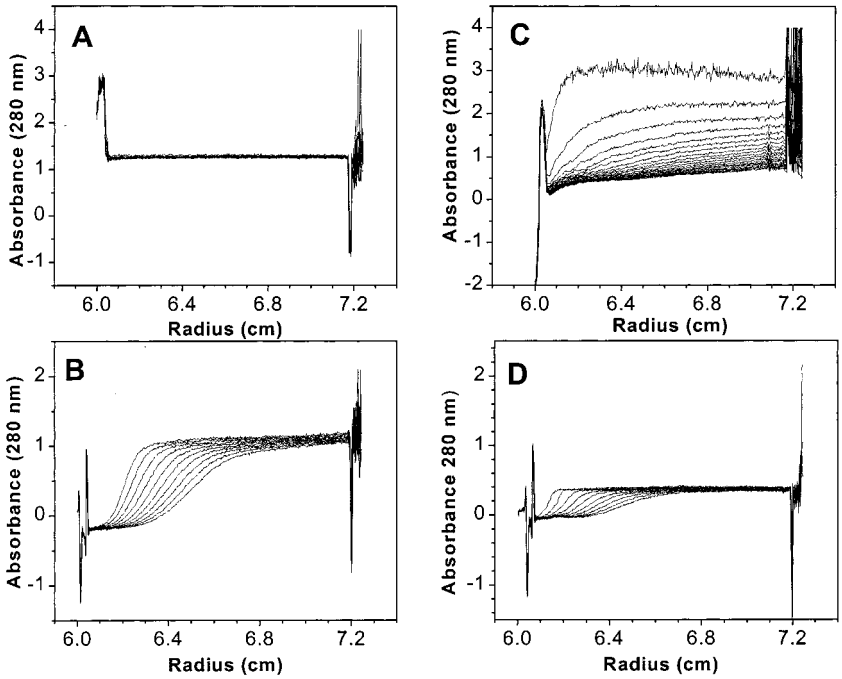

FIGURE 4: Sedimentation of lysozyme in the presence or absence of PDI. Reduced, denatured lysozyme (50 μM final concentration) was subjected to analytical centrifugation immediately after dilution into 100 mM HEPES, 20 mM NaCl, 2 mM EDTA, 5 mM $MgCl_2$, pH 7.0, containing 10 mM DTT and various amounts of PDI. The temperature was maintained at 25 °C. (A) Sedimentation of lysozyme in the absence of PDI at low speed (1500 rpm). (B) Sedimentation of lysozyme in the absence of PDI at high speed (42 000 rpm). (C) Sedimentation of lysozyme (50 μM) and PDI (2.5 μM) at low speed (1500 rpm). (D) Sedimentation of lysozyme (50 μM) and PDI (2.5 μM) at high speed (42 000 rpm). Individual scans of absorbance at 280 nm were taken at 70 s intervals along the length of the cell.

Table 1: Sedimentation Coefficients for Soluble and Insoluble Species in the Presence of PDI[a]

	large insoluble aggregate (1500 rpm)		soluble aggregates (42 000 rpm)	
[PDI] (μM)	S[b] (Svedberg)	MW (kDa)	S[b] (Svedberg)	MW (kDa)
0	ND[c]		19 ± 4	500
0.5	1000	190 000	19 ± 4	500
1.0	$7{,}800 \pm 500$	4×10^6	23 ± 5	660
1.5	$12{,}000 \pm 3{,}000$	8×10^6	25 ± 1	750
2.5	$17{,}000 \pm 9{,}000$	13×10^6	26 ± 1	800
5.0	$38\,000 \pm 14\,000$	44×10^6	ND[c]	ND[c]

[a] Aggregation was performed at a final lysozyme concentration of 50 μM at pH 7.0, 25 °C in 100 mM HEPES, 20 mM NaCl, 2 mM EDTA, 5 mM $MgCl_2$, 10 mM DTT, and various amounts of PDI. Large insoluble aggregates are those that sediment at 1500 rpm. Soluble aggregates are species that sediment only at higher speed (42 000 rpm). Apparent molecular mass was calculated assuming a spherical shape as described in Materials & Methods. [b] Average of duplicate or triplicate independent determinations. [c] Not detected.

the absorbance difference between the end of the 1500 rpm spin and the beginning of the 42 000 rpm spin. These are designated as "intermediate" aggregates (open squares). Again, at zero added PDI, little lysozyme (<4%) is found in intermediate aggregates. Next, "soluble" aggregates sediment during the high velocity spin (42 000 rpm). The amount of soluble aggregates is determined from the absorbance change near the top of the cell between the beginning and the completion of the 42 000 rpm spin. It represents species that sediment significantly at 42 000 rpm (23 S species). In the absence of PDI, the majority of the lysozyme sediments as soluble aggregates (open circles). Molecules that do not sediment by the end of the fast spin are designated as small, soluble species. They are detected by a constant, nonzero baseline (Figure 4, panel B). In the absence of PDI, little

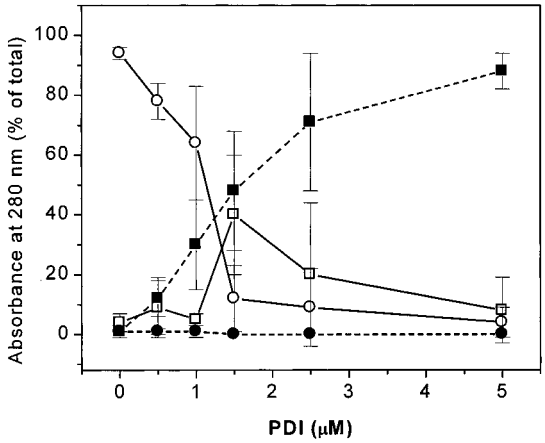

FIGURE 5: Partitioning among various sized species as a function of the PDI concentration. Aggregation was induced by adding reduced, denatured lysozyme (50 μM) to various concentrations of PDI in the ultracentrifuge. Experiments were performed at 25 °C in 100 mM HEPES, 20 mM NaCl, 2 mM EDTA, 5 mM $MgCl_2$, pH 7.0, containing 10 mM DTT. The amount of lysozyme in different sized species was calculated from the absorbance of 50 μM lysozyme (100%) and the residual absorbance at the end of spins at different speeds. Insoluble aggregates (■) are very large and are formed (see Figure 4) and removed at a low speed (1500 rpm). Intermediate aggregates (□) sediment during the acceleration of the rotor from 1500 to 42 000 rpm. The 23 S species (○) represent soluble aggregates that sediment at 42 000 rpm. In the absence of PDI, almost all of the protein is present in soluble aggregates. A small amount of lysozyme is found as small soluble species (●). Averages and standard deviations were computed from multiple, independent experiments.

lysozyme (2%) is found in this small, soluble fraction (filled circles).

As different concentrations of PDI are added, the distribution of lysozyme among the various aggregates changes.

With increasing PDI, the amount of soluble aggregates (open circles) clearly decreases. At the same time, large aggregates increase dramatically (filled squares). The amount of intermediate aggregates increases up until 1.5 μM PDI; higher PDI concentrations convert these species into the larger and insoluble aggregates. Higher antichaperone increments of PDI represent a threshold beyond which virtually all of the lysozyme and PDI are found in extremely large, insoluble aggregates at the expense of all other species.

Table 1 shows the approximate sedimentation coefficients and the corresponding molecular weights (assuming a spherical shape) of the soluble and insoluble aggregates formed at various concentrations of PDI and 50 μM lysozyme. While PDI has no significant effect on the size of soluble aggregates, the size of the insoluble species increases dramatically with increasing PDI. The largest insoluble entities have an estimated molecular mass on the order of 10^{10} Da. SDS-PAGE shows that both PDI and lysozyme are present in these aggregates (Figure 1). Antichaperone concentrations of PDI selectively deplete soluble, lysozyme-only species, by noncovalently cross-linking soluble aggregates of lysozyme into very large, insoluble entities that contain both proteins.

The time-dependent decrease in the absorbance at 280 nm observed between successive scans during the 1500 rpm spin (Figure 4C) can be used to monitor the rate of insoluble aggregate formation. The disappearance of material between successive scans is accurately described by a first-order exponential decay of the absorbance near the top of the cell vs time (data not shown). The rate constants for insoluble aggregate formation show a nonlinear dependence on the concentration of PDI, suggesting an initial high-order dependence on PDI concentration. At concentrations of PDI near the solubility minimum, the rate saturates and becomes PDI-independent (Figure 6A). Similar experiments varying the initial lysozyme concentration (10−50 μM) at a constant PDI concentration (1.5 μM) show that the rate constant for insoluble aggregate formation decreases with increasing lysozyme concentration. Like PDI, lysozyme aggregates at high concentration appear to inhibit further aggregation and divert protein away from the PDI-dependent aggregation pathway.

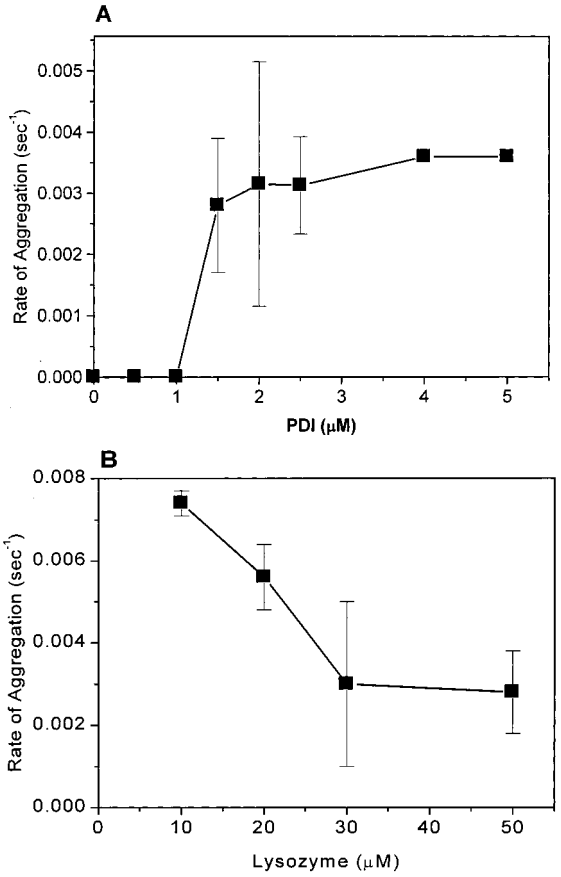

FIGURE 6: Dependence of the rate of PDI-induced lysozyme aggregation on PDI and lysozyme concentrations. The rate constant for the formation of insoluble aggregate formation was determined from the decrease in absorbance at 280 nm at a radial position of 6.3 cm in the ultracentrifuge cuvette during a 1500 rpm spin in sedimentation velocity experiments. Reduced, denatured lysozyme was diluted into 100 mM HEPES, 20 mM NaCl, 2 mM EDTA, 5 mM $MgCl_2$, pH 7.0, containing 10 mM DTT and various amounts of PDI. This decrease in absorbance between successive scans (see Figure 4) represents material that has formed and sedimented to the bottom of the cell during the 70 s scan. Plots of absorbance vs time were fitted as first-order exponential decays. (A) Dependence on the concentration of PDI (50 μM lysozyme). (B) Dependence on the concentration of lysozyme (1.5 μM PDI).

DISCUSSION

Partitioning Between Productive Folding and Aggregation. Goldberg et al. have found that during the oxidative refolding of lysozyme in the absence of PDI, the reduced, denatured lysozyme molecules kinetically partition between aggregation and productive folding pathways involving disulfide formation (*28*). The initial partitioning between folding and aggregation is fast (seconds); only lysozyme molecules that commit to fold during this short period will ultimately produce native lysozyme. Over the concentration range 10−50 μM, most of the lysozyme is present as an ensemble of large, soluble aggregates (23 ± 5 S) (Figure 4B). Once it enters the 23 S species, lysozyme cannot be productively folded, at least in vitro. Adding redox buffer and/or PDI after lysozyme has partitioned between different fates simply introduces intramolecular cross-links without generating native lysozyme (*19*). Thus, the 32% of the lysozyme that commits to productive folding in the absence of PDI, must partition quickly to disulfide-containing species that have lost affinity for being incorporated into this dead-end ensemble of soluble aggregates.

Depending on its concentration, PDI has different effects on the partitioning of refolding proteins between productive refolding and aggregation (*19, 21, 38*). At high concentrations, PDI behaves as a chaperone and inhibits aggregation, but at low concentrations, it can facilitate aggregation and divert proteins that would normally fold into large, insoluble aggregates. We have previously shown (*19*) that it takes up to 50−100 μM PDI and a redox buffer to promote the complete (>90%) conversion of 10 μM lysozyme to the native enzyme. However, as can be seen in Figure 1, much lower concentrations of PDI (5−10 μM) will maintain lysozyme in a soluble state without facilitating its refolding or its aggregation (90% soluble, but only 35% native, Figure 1). The absence of a direct correspondence between solubility and regain of lysozyme activity (Figure 1) requires the existence of a soluble lysozyme species that cannot be refolded—presumably the 23 S species, since they are the dominant, soluble lysozyme species and are resistant to refolding. Very high concentrations of PDI are evidently

necessary to compete kinetically with 23 S species formation and to prevent monomeric lysozyme from entering this dead-end misfolding pathway.

When PDI is present at low concentrations relative to lysozyme, it acts as an antichaperone, facilitates aggregation, and decreases the yield of native protein (Figure 1) (*19*) by diverting lysozyme into large, insoluble aggregates that contain both lysozyme and PDI (Figure 3). The catalytic activity of PDI is not required to induce aggregation (*20*) nor does disulfide formation contribute significantly to aggregate formation; when disulfide formation is inhibited by including high concentrations of DTT, PDI still directs lysozyme toward aggregation (Figure 1B).

Size and Composition of Insoluble Lysozyme Aggregates. The insoluble aggregates resulting from antichaperone behavior contain PDI and lysozyme at defined ratios. For a range of lysozyme concentrations (10−50 μM), maximal amounts of insoluble aggregates are consistently observed at a lysozyme to PDI ratio near 10:1 under both oxidizing (data not shown) and reducing (Figure 2) conditions. The two proteins in these aggregates are resolubilized to approximately the same extent by increasing concentrations of urea, suggesting that both proteins are integral members of the aggregate and that PDI does not simply coprecipitate with an insoluble form of lysozyme nor absorb on the surface of lysozyme aggregates (Figure 3). Although disulfide bonds have been detected in lysozyme-only (*39*) as well as PDI−lysozyme (*19*, *20*) aggregates, disulfide cross-links are clearly not needed to form insoluble, mixed aggregates. Disulfides make the aggregate more resistant to solubilization by urea but do not participate directly in its formation. The consistent stoichiometry at the solubility minimum and the inability to induce lysozyme aggregation with control proteins (*19*) argue that the 23 S species are cross-linked into a large, insoluble network through relatively specific interactions with PDI.

Mechanism of Aggregation. Analytical ultracentrifugation provides additional structural information on the aggregation of lysozyme by itself and on PDI−lysozyme aggregates. In the absence of PDI, reduced lysozyme clusters into an array of large, soluble aggregates. Heterogeneity analysis (*40*, *41*) for these soluble species reveals a range of sedimentation coefficients between 12 and 30 S (data not shown) for all concentrations of lysozyme examined (10−50 μM).

This population of lysozyme aggregates sediments with an average coefficient of 23 ± 5 S and an estimated molecular mass of 600 ± 100 kDa. These soluble clusters, containing anywhere from 30 to 50 lysozyme molecules, represent a sizable fraction (59%) of the total lysozyme, even at low lysozyme concentrations (10 μM); almost all of the lysozyme (92%) is present in these species at a total concentration of 50 μM.

Low, antichaperone concentrations of PDI convert the soluble 23 S lysozyme aggregates into higher molecular weight species, which sediment at low speeds (1500 rpm). With increasing amounts of PDI, more and more lysozyme is assimilated into aggregates that grow increasingly large (Figure 5, Table 1); these aggregate networks can grow to a size of >38 000 S (10^{10} daltons). The enormous sizes measured for the PDI−lysozyme aggregate networks are not unusual; similar species have been observed during the sedimentation of the Aβ amyloidogenic peptide under conditions associated with amyloid formation (*37*).

The rate of insoluble aggregate formation is very slow at low PDI concentrations, suggesting that there is some intermediate that must accumulate before aggregation can proceed (Figure 6A). The cooperative nature of this transition implies that multiple PDI molecules are involved in its formation, but the precision with which the aggregation rates can be measured precludes an accurate estimation of the numbers of PDI involved. This cooperative behavior of PDI should not be confused with the nucleation commonly observed for amyloid formation. Nucleation events lead to a lag in aggregate formation with time (*42*), and here, aggregation is first-order. As the PDI concentration approaches that required to maximally aggregate the lysozyme, the rate of the process becomes PDI-independent, implying a limited number of binding sites for PDI on the 23 S lysozyme species that can be occupied to cross-link multiple aggregates. A limited number of binding sites is also consistent with a constant lysozyme/PDI stoichiometry in the insoluble aggregates. The eventual ratio within mixed aggregates is 10 molecules of lysozyme per molecule of PDI. Assuming that the 23 S species (40 lysozyme molecules on average) is the species that is cross-linked, there may be as many as four PDI molecules surrounding each particle in the network lattice. The exact binding arrangement will depend on the structure of the aggregate. At even higher PDI concentrations, the extent of aggregation declines (Figure 1) suggesting that the PDI-dependent aggregation of the 23 S species can be inhibited by high PDI concentrations. The dependence of the aggregation rate on the lysozyme concentration (Figure 6 B) shows that increasing lysozyme decreases the rate of aggregate formation, at least at the concentrations that could be examined in the ultracentrifuge. Either a soluble complex of 23 S species accumulates that is not cross-linked by PDI or an excess of the 23 S species inhibits PDI-dependent aggregation.

The aggregation mechanism shown in Figure 7 is the simplest one that accounts for the antichaperone and chaperone activities of PDI against lysozyme as well as the inhibition of aggregation by high concentrations of either PDI or lysozyme (23 S). The central feature is that aggregation occurs through a network of 23 S species cross-linked by multiple interactions with PDI. Network formation would require an optimum concentration of PDI and 23 S species. At high chaperone concentrations of PDI, the 23 S species become saturated with PDI so that available sites on other 23 S species would be difficult to find. Aggregation should saturate with increasing PDI concentration and then decrease as PDI begins behaving as a chaperone that covers the available 23 S sites (Figure 7, lower path). Changing the concentration of 23 S species should have a similar overall effect on the aggregation rate. At low lysozyme, the rate should increase as more unoccupied 23 S species become available, saturate, and then decrease as all of the sites on the PDI become occupied with 23 S species (Figure 7, upper path). The decrease in aggregation rate with increasing lysozyme concentration (Figure 6) is consistent with this feature of the mechanism. At sufficiently low lysozyme concentrations (1−10 μM), the rate should increase with increasing lysozyme; however, it is not possible to examine lysozyme concentrations below 10 μM in the ultracentrifuge. It should be noted that we do not have direct evidence for the accumulation of the two soluble lysozyme aggregates

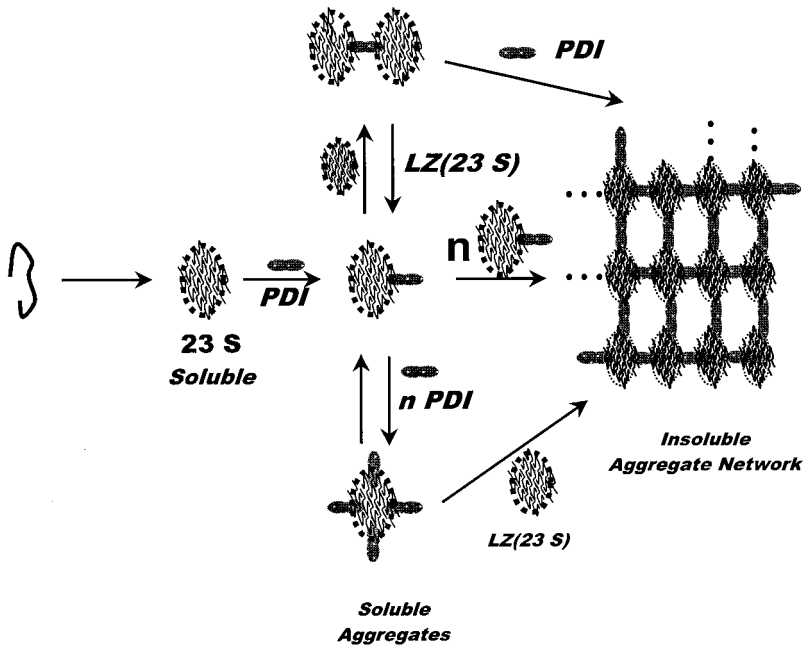

FIGURE 7: Mechanism of lysozyme aggregation. Monomeric, denatured lysozyme rapidly aggregates into a relatively uniform ensemble of 23 S species containing approximately 40 lysozyme molecules. Multiple interactions between PDI and lysozyme result in cross-linking the proteins into a large insoluble network. Formation of insoluble aggregates requires open binding sites on both PDI and lysozyme. A large excess of lysozyme (23 S) will inhibit aggregation by removing the free PDI required to establish new cross-links. A large excess of PDI will remove free 23 S species and inhibit aggregation. For simplicity, the stoichiometry is illustrated as four PDI molecules per 23 S species and two 23 S species per PDI.

cross-linked by a PDI molecule, which we believe to be intermediates in the aggregation pathway (Figure 7, upper path), possibly due to their low steady-state levels during the formation of large, insoluble aggregates. In summary, at optimal concentrations (minimum solubility), the PDI−lysozyme interactions cross-link smaller, soluble aggregates into large and insoluble networks via noncovalent association. The process is reminiscent of immunoprecipitation of a multivalent antigen by bivalent antibodies.

Aggregation and Amyloid Formation. Protein aggregation plays a central role in the onset of many diseases, notably amyloid and prion diseases (*1*−*3*). The major component of neuritic plaques observed in Alzheimer's disease is the peptide amyloid-β (Aβ), a cleavage product of the amyloid presursor protein (*43*). While soluble Aβ is nontoxic, it plays a pathological role in its aggregated form. Snyder et al. have described a mechanism for aggregation of Aβ very similar to the one observed with PDI−lysozyme. A cleaved form of this peptide produces two types of species: large, insoluble aggregates of ~50 000 S and soluble aggregates of ~30 S (*37*). These insoluble aggregates were shown by electron microscopy to consist of densely packed, amyloid-like fibrils (*37*).

A mechanistic link between amyloidogenesis and the PDI-mediated cross-linking of lysozyme aggregates into large networks is particularly pertinent in view of recent findings on the involvement of lysozyme in amyloid disease and the suggestion that chaperones can participate directly in vitro (*19*−*21*) or indirectly (*9*) in aggregate formation. Naturally occurring mutations in the human lysozyme gene are associated with hereditary amyloidosis (*33*). The lysozyme variants readily cause amyloid fibril formation upon heating (*6*). Aggregation is thought to involve the transient population of a soluble, partially folded, molten globule-like intermediate in the folding of lysozyme (*6*, *34*). Fibrils are proposed to grow as multiple molecules of the folding intermediate associate via their unstable β-domains (*6*). While there have been no reports of an association between wild-type human lysozyme and PDI, PDI has been found associated with a misfolded human lysozyme variant in vivo (*27*). We have no evidence that the insoluble PDI−lysozyme aggregates are amyloid in nature; however, the possibility is under investigation. Although aggregation has traditionally been viewed as arising from nonspecific interactions, it is clear that specific interactions between folding intermediates and/or misfolded proteins may be responsible for the multiple interactions leading to the formation of large, insoluble aggregates (*44*).

Aggregation and "Quality Control". Association of aggregates with molecular chaperones in vivo may be a fairly common cellular phenomenon. The formation of aggregates in inclusion bodies or aggresomes (*45*) within the cell during protein overexpression is well-documented. For some proteins, aggregation may even be a normal stage following biosynthesis (*17*) or serve as a route to degradation (*18*). In the ER, proteins are retained as disulfide-linked or reduced aggregates by local chaperones such as BiP under conditions of cellular stress (*23*, *24*). The antichaperone activities of PDI and BiP that we have found in vitro may be a manifestation of how ER chaperones have evolved to perform multiple duties in this highly specialized folding compartment of the cell.

ACKNOWLEDGMENT

We would like to thank the laboratories of Drs. K. S. Matthews and S. J. Olson at Rice University for graciously allowing us to use the XL-A analytical ultracentrifuge, and Borries Demeler, University of Texas Health Science Center, for use of the UltraScan 4.1 software.

REFERENCES

1. Lansbury, P. T. (1999) *Proc. Natl. Acad. Sci. U.S.A. 96*, 3342−4.
2. Kelly, J. W. (1998) *Proc. Natl. Acad. Sci. U.S.A. 95*, 930−2.
3. Prusiner, S. B. (1998) *Proc. Natl. Acad. Sci. U.S.A. 95*, 13363−83.
4. Conway K. A., Harper, J. D., and Lansbury, P. T. (1998) *Nat. Med. 4*, 1318−20.
5. Lashuel H. A., Lai, Z., and Kelly, J. W. (1998) *Biochemistry 37*, 17851−64.
6. Booth, D. R., Sunde, M., Bellotti, V., Robinson, C. V., Hutchinson, W. L., Fraser, P. E., Hawkins, P. N., Dobson, C. M., Radford, S. E., Blake, C. C. F., and Pepys, M. B. (1997) *Nature 385*, 787−93.
7. Sunde, M., Serpell, L. C., Bartlam, M., Fraser, P. E., Pepys, M. B., and Blake, C. C. F. (1997) *J. Mol. Biol. 273*, 729−39.
8. Lundberg, K. M., Stenland, C. J., Cohen, F. E., Prusiner, S. B., and Millhauser, G. L. (1997) *Chem. Biol. 4*, 345−55.
9. Lindquist, S. (1997) *Cell 89*, 495−8.
10. Yang, Y., Turner, R. S., and Gaut, J. R. (1998) *J. Biol. Chem. 273*, 25552−5.
11. Liautard J. P. (1994) *Med. Hypotheses 43*, 372−80.
12. Ma, J., Yee, A., Brewer, H. B., Jr., Das, S., and Potter, H. (1994) *Nature 372*, 92−4.
13. Beissinger, M., and Buchner, J. (1998) *Biol. Chem. 379*, 245−59.
14. Carrio, M. M., Corchero, J. L., and Villaverde, A. (1998) *FEMS Microbiol. Lett. 169*, 9−15.
15. Arias, A. E., Velez-Granell, C. S., Torres-Ruiz, J. A., and Bendayan, M. (1994) *Exp. Cell Res. 215*, 1−8.
16. Bova, M. P., Yaron, O., Huang, Q., Ding, L., Haley, D. A., Stewart, P. L., and Horwitz, J. (1999) *Proc. Natl. Acad. Sci. U.S.A. 96*, 6137−42.
17. Kim, P. S., Bole, D., and Arvan, P. J. (1992) *Cell Biol. 118*, 541−9.
18. Cotner, T., and Pious, D. (1995) *J. Biol. Chem. 270*, 2379−86.
19. Puig, A., and Gilbert, H. F. (1994) *J. Biol. Chem. 269*, 7764−71.
20. Puig, A., Lyles, M. M., Noiva, R., and Gilbert, H. F. (1994) *J. Biol. Chem. 269*, 19128−35.
21. Puig, A., and Gilbert, H. F. (1994) *J. Biol. Chem. 269*, 25889−96.
22. Song, J., Quan, H., and Wang, C. C. (1997) *Biochem. J. 328*, 841−6.
23. Marquardt, T., and Helenius, A. (1992) *J. Cell. Biol. 117*, 505−13.
24. Braakman, I., Helenius, J., and Helenius, A. (1992) *Nature 356*, 260−2.
25. deSilva, A., Braakman, I., and Helenius, A. (1993) *J. Cell. Biol. 120*, 647−55.
26. Lodish, H. F., and Kong, N. (1993) *J. Biol. Chem. 268*, 20598−605.
27. Otsu, M., Omura, F., Yoshimori, T., and Kikuchi, M. (1994) *J. Biol. Chem. 269*, 6874−7.
28. Goldberg, M. E., Rudolph, R., and Jaenicke, R. (1991) *Biochemistry 30*, 2790−7.
29. Matagne, A., Radford, S. E., and Dobson, C. M. (1997) *J. Mol. Biol. 267*, 1068−74.
30. Matagne, A., Chung, E. W., Ball, L. J., Radford, S. E., Robinson, C. V., and Dobson, C. M. (1998) *J. Mol. Biol. 277*, 997−1005.
31. Morgan, C. J., Miranker, A., and Dobson, C. M. (1998) *Biochemistry 37*, 8473−80.
32. Eyles, S. J., Radford, S. E., Robinson, C. V., and Dobson, C. M. (1994) *Biochemistry 33*, 13038−48.
33. Pepys, M. B., Hawkins, P. N., Booth, D. R., Vigushin, D. M., Tennent, G. A., Soutar, A. K., Totty, N., Nguyen, O., Blake, C. C., and Terry, C. J. (1993) *Nature 362*, 553−7.
34. Canet, D., Sunde, M., Last, A. M., Miranker, A., Spencer, A., Robinson, C. V., and Dobson, C. M. (1999) *Biochemistry 38*, 6419−27.
35. Gilbert, H. F., Kruzel, M. L., Lyles, M. M., and Harper, J. W. (1991) *Prot. Exp. Purif. 2*, 194−8.
36. Bradford, M. (1976) *Anal. Biochem. 72*, 248−54.
37. Snyder, S. W., Ladror, U. S., Wade W. S., Wang, G. T., Barret, L. W., Matayoshi, E. D., Huffaker, H. J., Krafft, G. A., and Holzman T. F. (1994) *Biophys. J. 67*, 1216−28.
38. Primm, T. P., Walker, K. W., and Gilbert, H. F. (1996) *J. Biol. Chem. 271*, 33664−69.
39. De Bernardez-Clark, E., Hevehan, D., Szela, S., and Maachupalli-Reddy, J. (1998) *Biotechnol. Prog. 14*, 47−54.
40. van Holde, K. E., and Weischet, W. O. (1978) *Biopolymers 17*, 1387−1403.
41. Demeler, B., Saber, H., and Hansen, J. C. (1997) *Biophys. J. 72*, 397−407.
42. Jarrett, J. P., and Lansbury, P. T., Jr. (1993) *Cell 73*, 1055−8.
43. Kosik, K. S. (1999) *Proc. Natl. Acad. Sci. U.S.A.* 96, 2574−6.
44. Speed, M. A., Wang, D. I., and King, J. (1996) *Nat. Biotechnol. 14*, 1283−1287.
45. Johnston, J. A., Ward, C. L., and Kopito, R. R.(1998) *J. Cell. Biol. 143*, 1883−1898.

BI992246Q